Spectrochimica Acta Part A 79 (2011) 672–679

Contents lists available at ScienceDirect

Spectrochimica Acta Part A: Molecular and Biomolecular Spectroscopy

journal homepage: www.elsevier.com/locate/saa

Intermolecular hydrogen bond complexes by *in situ* charge transfer complexation of o-tolidine with picric and chloranilic acids

Moamen S. Refat[a,b,*], Hosam A. Saad[b,c], Abdel Majid A. Adam[b]

[a] *Department of Chemistry, Faculty of Science, Port Said, Port Said University, Egypt*
[b] *Department of Chemistry, Faculty of Science, Taif University, 888 Taif, Saudi Arabia*
[c] *Department of Chemistry, Faculty of Science, Zagazig University, Zagazig, Egypt*

ARTICLE INFO

Article history:
Received 27 January 2011
Received in revised form 28 March 2011
Accepted 31 March 2011

Keywords:
o-Tolidine (o-TOL)
^{13}C NMR
^{1}H NMR
Charge transfer
Thermal analysis

ABSTRACT

A two new charge transfer complexes formed from the interactions between o-tolidine (o-TOL) and picric (PA) or chloranilic (CA) acids, with the compositions, [(o-TOL)(PA)$_2$] and [(o-TOL)(CA)$_2$] have been prepared. The ^{13}C NMR, ^{1}H NMR, ^{1}H-Cosy, and IR show that the charge-transfer chelation occurs *via* the formation of chain structures O–H···N intermolecular hydrogen bond between 2NH$_2$ groups of o-TOL molecule and OH group in each PA or CA units. Photometric titration measurements concerning the two reactions in methanol were performed and the measurements show that the donor–acceptor molar ratio was found to be 1:2 using the modified Benesi–Hildebrand equation. The spectroscopic data were discussed in terms of formation constant, molar extinction coefficient, oscillator strength, dipole moment, standard free energy, and ionization potential. Thermal behavior of both charge transfer complexes showed that the complexes were more stable than their parents. The thermodynamic parameters were estimated from the differential thermogravimetric curves. The results indicated that the formation of molecular charge transfer complexes is spontaneous and endothermic.

1. Introduction

The charge transfer interactions of significant interactions, which have many applications in various fields, therefore, received considerable attention in recent years by many researchers [1–5]. CT complexes have applications in many fields such as electronics, solar cells [6], optical devices and electrical conductivities [7]. Charge transfer complexes have also been recognized as an important phenomenon in drug receptor binding mechanism and in many biological processes like photosynthesis and oxidative processes [8]. The charge transfer reactions have successfully utilized in pharmaceutical analysis as given the drug (donor) with different acceptors [9–12].

o-Tolidine (Formula I) is slightly soluble in water and has a melting point of 129 °C. It readily forms salts with acids [13]. o-Tolidine is a commercially important aromatic amines used mainly for dye production, but also for the production of certain elastomers. o-Tolidine is an intermediate for the production of soluble azo dyes and insoluble pigments used particularly in the textile, leather and paper industries [14]. Also it is widely used as a reagent or indicator in analytical, clinical and forensic chemistry, such as in the analytical determination of gold. Numerous studies have been [15,16] devoted to aromatic amines suspected of having mutagenic or carcinogenic properties.

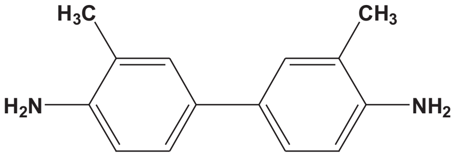

In continuation of our aimed studies on such type of interactions [17–20], herein this paper was reported the spectral tools in order to investigate the intermolecular hydrogen bond of the charge transfer complexes of o-tolidine (o-TOL) with picric (PA) and chloranilic (CA) acids. A literature survey reveals that no work on the formation of charge transfer complexes between o-tolidine and either PA or CA acids have been investigated. In view of this, we described the synthesis and spectroscopic characterizations such as UV–vis, FT-IR, ^{1}H NMR, ^{13}C NMR and ^{1}H-Cosy in the present study to interpretative the mechanism of interaction of o-tolidine with PA and CA acceptors. To track the status of the thermal stability of charge transfer complexes formed the thermo gravimetric/differential thermo gravimetric analysis and kinetic thermodynamic parameters (E^*, ΔS^*, ΔH^* and ΔG^*) were employed.

---

* Corresponding author at: Department of Chemistry, Faculty of Science, Taif University, 888 Taif, Saudi Arabia. Tel.: +966 561926288.
E-mail address: msrefat@yahoo.com (M.S. Refat).

1386-1425/$ – see front matter © 2011 Elsevier B.V. All rights reserved.
doi:10.1016/j.saa.2011.03.058

2. Experimental

o-Tolidine (o-TOL) was of analytical reagent grade (Aldrich Co.). Both π-acceptors (PA and CA) were purchased from Aldrich. Stock solutions of o-TOL and acceptors were freshly prepared and the spectroscopic grade methanol (BDH) was used as received.

2.1. Synthesis of o-TOL/PA and o-TOL/CA charge-transfer complexes

The two solid CT-complexes of o-TOL with PA or CA were prepared by mixing a saturated solution of the o-TOL donor in 10 ml MeOH to each of saturated solutions of PA or CA in the same solvent with continuously stirring for about 45 min at room temperature. The solutions were allowed to evaporate slowly at room temperature, the resulted complexes in the solid state filtered and washed several times with little amounts of solvent, and dried under vacuum over anhydrous calcium chloride. Charge-transfer complexes of o-TOL/PA formed with empirical formula $C_{26}H_{22}N_8O_{14}$ with molecular weight 670.5 g/mol and o-TOL/CA formed with empirical formula $C_{26}H_{20}N_2Cl_4O_8$ with molecular weight 630.3 g/mol.

$[(\text{o-TOL})(\text{PA})_2]$: Color: yellow, yield: 84%, Calc. (%): C = 46.53%, H = 3.28% and N = 16.70%, Found (%): C = 46.34%, H = 3.21% and N = 16.47%.
$[(\text{o-TOL})(\text{CA})_2]$: Color: violet, yield: 87%, Calc. (%): C = 49.50%, H = 3.17% and N = 4.44%, Found (%): C = 49.27%, H = 3.13% and N = 4.35%.

2.2. Analysis

The electronic UV–vis. spectra of the o-TOL, PA, CA and the resulted CT complexes were recorded in the region of (200–800 nm) by using a Jenway 6405 Spectrophotometer with quartz cells, 1.0 cm path in length. IR measurements (KBr discs) of the o-TOL, acceptor and both CT complexes were carried out on a Bruker FT-IR spectrophotometer (400–4000 cm^{-1}). The NMR spectra were obtained on a Bruker DRX-250 spectrometer, operating at 250.13 and 62.90 MHz for ^1H and ^{13}C, respectively using a dual 5 mm probe head. The measurements were carried out in DMSO-d_6 solution at ambient temperature. The chemical shift was referenced to tetramethylsilane (TMS), standard experiments with 30° pulses, 1 s relaxation delays, 16 K time domain points, zero-filled to 64 K for protons and 32 K for carbons were performed. The distortionless enhancement by polarization transfer (DEPT) spectra were recorded under the same conditions as the ^{13}C NMR spectra and $\tau = (2^1J_{CH}) - 1 = 3.45$ μs was used. The 2D $^1H/^1H$ correlated spectra (COSY) were performed with spectral width 2200 Hz, relaxation delay 2 s, number of increments 512, and size 1 K × 1 K. The 2D $^1H/^{13}C$ heteronuclear multiple quantum coherence (HMQC) experiments were carried out with a spectral width of 2200 Hz for ^1H and 9000 Hz for ^{13}C, relaxation delay 1.5 s, FT size 1 K × 256 W. The thermal analysis (TGA/DTG) was carried under nitrogen atmosphere with a heating rate of 10 C/min using a Shimadzu TGA-50H thermal analyzers.

3. Results and discussion

3.1. UV–vis spectral studies

UV–vis absorption spectra of o-TOL/PA and o-TOL/CA CT-complexes were scanned in MeOH solvent. The concentration of o-TOL in the reaction mixture was kept fixed at 1.0×10^{-4} M in MeOH solvent, while, the concentration of PA or CA was changed from 0.25×10^{-4} M to 4.0×10^{-4} M. These concentrations were covered along the range from 1:0.25 to 1:4.00. The UV–vis spectra of o-TOL/PA and o-TOL/CA systems were shown in Fig. 1A and B. The measured spectra were detected definite absorption bands which are not existed in both spectra of the free donor and acceptors. These bands are noticed at (352 and 419 nm) and (335 and 532 nm) due to CT-complexes formed from the reactions of o-TOL with PA and CA, respectively. Photometric titration curves based on charge transfer bands are shown in Fig. 2A and B. These photometric titration curves were obtained according to well known method [21] and it is refereed to formation of 1:2 CT complexes. The 1:2 Eq. (1) [22] was used in the calculations.

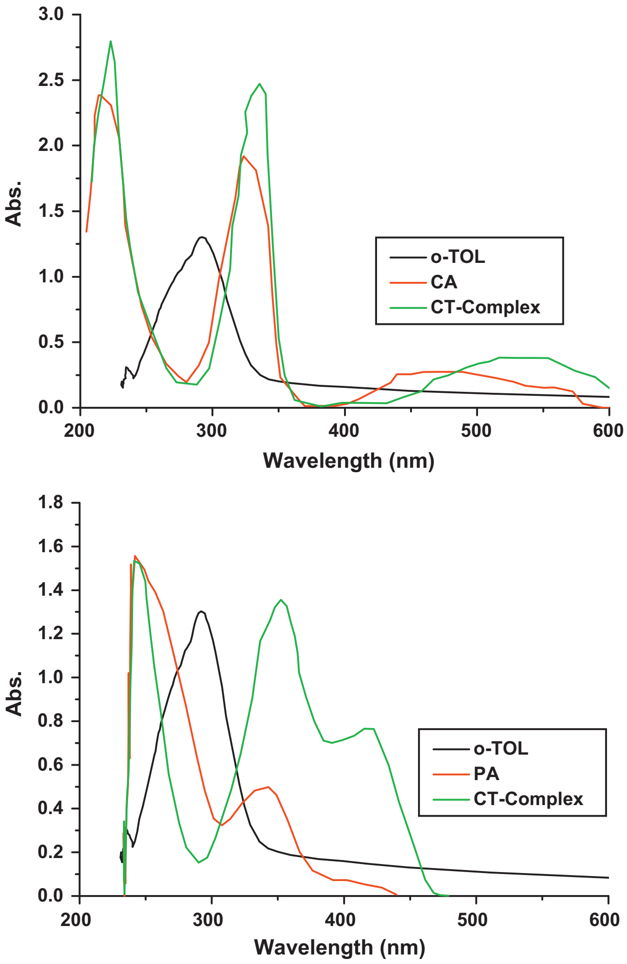

Fig. 1. Electronic absorption spectra of o-TOL/CA and o-TOL/PA reactions in MeOH.

$$\frac{C_A^{\circ 2} C_D^{\circ}}{A} = \frac{1}{K\varepsilon} + \frac{1}{\varepsilon}.C_A^{\circ}(4C_D^{\circ} + C_A^{\circ}) \qquad (1)$$

where $C_A^{\circ 2}$ and C_2° are the initial concentration of the π-acceptor (PA and CA) and donor (o-TOL), respectively, and A is the absorbance of the detected CT-band. The data obtained C_D°, $C_A^{\circ 2}$, $C_A^{\circ}(4C_D^{\circ} + C_A^{\circ})$ and $(C_A^{\circ 2}.C_D^{\circ})/A$ in methanol were calculated. By plotting $(C_A^{\circ 2}.C_D^{\circ})/A$ values vs $C_A^{\circ}(4C_D^{\circ} + C_A^{\circ})$, straight lines were obtained with a slope of $1/\varepsilon$ and an intercept of $1/k\varepsilon$ as shown in Fig. 3A and B.

The oscillator strength f was obtained from the approximate formula [23].

$$f = (4.319 \times 10^{-9})\varepsilon_{\max}.\nu_{1/2} \qquad (2)$$

where $\nu_{1/2}$ is the band-width for half-intensity in cm^{-1} and $\varepsilon_{\max}$ is the maximum extinction coefficient of the CT-band. The oscillator strength values are given in Table 1. The data resulted reveals

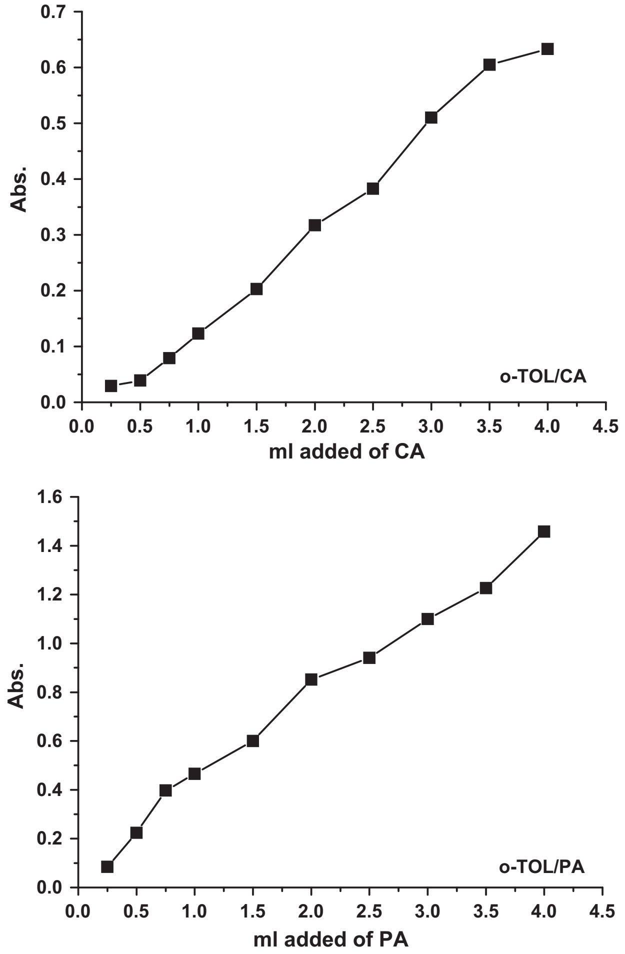

Fig. 2. Photometric titration curves for the o-TOL/CA and o-TOL/PA systems at 532 and 419 nm, respectively.

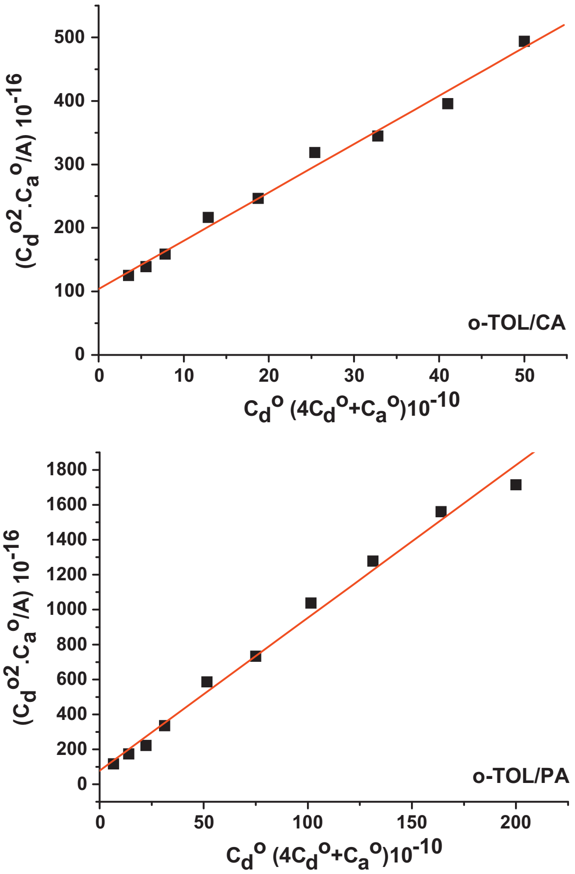

Fig. 3. The plot of $C_d{}^{\circ}\,(4\,C_d{}^{\circ}+C_a{}^{\circ})$ values against $(C_d{}^{\circ 2}{\cdot}C_a{}^{\circ}/\mathrm{A})$ values for the o-TOL/CA and o-TOL/PA systems at 532 and 419 nm, respectively.

several items. (i) The o-TOL/PA and o-TOL/CA systems show high values of both formation constant (K) and molar absorptivity (ε). This high value of (K) reflects the high stability of the o-TOL complexes as a result of the expected high donation of the o-TOL which contains two of amino and methyl groups. (ii) The different values of the oscillator strength, f, increases with increasing in the dielectric constant (D) of the solvent. This result could be explained on the basis of competitive solvent interactions with the acceptors [24,25].

The transition dipole moment (μ) of the o-TOL CT-complexes, Table 1, has been calculated from Eq. (3) [26];

$$m(\mathrm{Debye}) = 0.0958[\varepsilon_{\max}\upsilon_{1/2}/\upsilon_{\max}]^{1/2} \tag{3}$$

The transition dipole moment is useful for determining if transitions are allowed, that the transition from a bonding π orbital to an antibonding π* orbital is allowed because the integral defining the transition dipole moment is nonzero.

The ionization potential (I_p) of the o-TOL donor in the charge transfer complexes of (o-TOL/PA and o-TOL/CA) are calculated using empirical equation derived by Aloisi and Piganatro Eq. (4) [27,28];

$$ID(ev) = 5.76 + 1.53 \times 10^{-4}\nu_{\mathrm{CT}} \tag{4}$$

where ν_{CT} is the wavenumber in cm^{-1} corresponding to the CT band formed from the interaction between donor and acceptor. The electron donating power of a donor molecule is measured by its ionization potential which is the energy required to remove an electron from the highest occupied molecular orbital.

The energy of the charge-transfer complexes E_{CT} of the o-TOL complexes is calculated using Eq. (5) [26];

$$E_{\mathrm{CT}} = (h\nu_{\mathrm{CT}}) = 1243.667/\lambda_{\mathrm{CT}}\ (\mathrm{nm}) \tag{5}$$

where, λ_{CT} is the wavelength of the complexation band.

Determination of resonance energy (R_N) [29] theoretically derived from (Eq. (6));

$$\varepsilon_{\max} = \frac{7.7 \times 10^{-4}}{h\nu_{CT}/[R_N - 3.5]} \tag{6}$$

where $\varepsilon_{\max}$ is the molar absorptivity of the CT-complexes at maximum CT band, ν_{CT} is the frequency of the CT peak and R_N is the resonance energy of the complex in the ground state, which, obviously is a contributing factor to the stability constant of the complex (a ground state property). The values of R_N for the (PA and CA) complexes under study have been given in Table 1.

Table 1
Spectrophotometric results of the o-TOL CT-complexes; (A) [(o-TOL)(CA)] and (B) [(o-TOL)(PA)].

Complex	$\lambda_{\max}$ (nm)	E_{CT} (eV)	K (l mol^{-1})	$\varepsilon_{\max}$ (l mol^{-1} cm^{-1})	f	μ	I_p	D	R_N	ΔG°(25 °C) (KJ mol^{-1})
A	532	2.34	0.073×10^{10}	0.1314×10^{6}	45.40	71.64	8.64	33	0.572	6.48×10^{13}
B	419	2.97	0.112×10^{10}	0.1143×10^{6}	49.37	66.30	9.41	33	0.711	5.43×10^{13}

The standard free energy changes of complexation (ΔG°) were calculated from the formation constants by the following Eq. (7) [30];

$$\Delta G^\circ = -2.303RT\ \log K_{CT} \tag{7}$$

where ΔG° is the free energy change of the CT-complexes (KJ mol^{-1}), R is the gas constant (8.314 J mol^{-1} K), T is the temperature in Kelvin degrees (273+ °C) and K_{CT} is the formation constant of the complexes (l mol^{-1}) in different solvents at room temperature.

3.2. *Infrared spectral studies*

Infrared spectral studies sheds light on the place of donation in donor species and the differences occurs in the spectra of both PA and CA charge transfer complexes. Comparison between the spectra of both CT-complexes and the data of o-TOL donor and receptors have been studied and recorded in Table 2. The full spectra of o-TOL/CA and o-TOL/PA were shown in Fig. 4A and B.

If we take into account the changes that have taken place in the region of 4000–3000 cm^{-1}, we find that this area includes some stretching vibration motions; the ν(OH) group of CA and PA acceptors, ν(N–H) of NH_2 group of o-TOL donor and some of stretching motions of ν(C–H) respected to the aromatic rings.

$$3412\,\text{s} + 3375\,\text{s} + 3338\,\text{ms}\,(\text{o-TOL free donor}) \rightarrow$$
$$3414\,\text{vw} + 3386\,\text{w} + 3357\,\text{vw}(\text{o-TOL/CA complex})$$
$$3400\,\text{s} + 3328\,\text{s}\,(\text{o-TOL/PA complex})$$

Found that the values characteristic of both the –OH and the $-NH_2$ groups happened to shifted to a lower values and also decreased in the intensities of vibration motions, which indicates that the interactions placed among the –OH group of each of CA and PA and $-NH_2$ group of o-TOL through the hydrogen bonding (region 3000–2000 cm^{-1}) existed at 2757 sh, 2643 w, 2571 w for o-TOL/CA and 2728 vw, 2657 vw, 2571 w, 2543 w for o-TOL/PA. These new bands were attributed to the stretching vibration of a proton attached to the donation site ($-NH_2$) of the donor and forming $^+NH_3$ group [31]. These results caused by the protonation of both NH_2 group of the o-TOL donor through one protons transfer from the acidic center on the CA or PA acceptors *via* –OH group to the basic center on the donor NH_2 group.

To place greater emphasis on the interactions between the donor and both acceptors, the 2000–1000 cm^{-1} region was investigated. This region contain the bending vibration motions of $-NH_2$ group ($\delta(NH_2)$) which influenced by charge transfer complexation

Table 2
Infrared frequencies[a] (cm^{-1}) and tentative assignments for o-TOL, CA, PA, [(o-TOL)(CA)], and [(o-TOL)(PA)] CT-complexes.

o-TOL	CA	PA	o-TOL/CA	o-TOL/PA	Assignments[b]
3475 s	3420 s,br	3416 br	3471 vw	3400 s	ν(O–H)
3412 s	3235 s, br	3103 ms	3414 vw	3328 s	ν(N–H); NH_2
3375 s			3386 w		
3338 ms			3357 vw		
3213 ms	–	2980 sh	3143 sh	3200 s,br	ν(C–H); aromatic rings
3019 m		2872 w		3114 sh	
				3057 w	
2982 ms	–	–	2957 vw	2986 vw	ν_s(C–H); CH_3
2940 mw			2914 vw	2929 vw	ν_{as}(C–H); CH_3
2898 w			2857 vs,br	2857 vw	
2856 w				2814 vw	
–	–	–	2757 sh	2728 vw	Hydrogen bonding
			2643 w	2657 vw	
			2571 w	2571 w	
				2543 w	
1870 ms	1664 ms	1861 ms	1618 s	1614 vs	Overtone of δ(CH)
1625 vs	1630 vs	1632 vs	1485 vs	1557 s	$\nu_{as}(NO_2)$; PA
1574 s		1608 vs		1528 s	ν(C=O) + ν(C=C)
1520 w		1529 vs		1486 vs	$\delta(NH_2)$
1489 m					Ring breathing bands
1458 s	1368 s	1432 s	1428 vw	1400 s	$\delta_{as}(CH_3) + \delta_s(CH_3)$
1384 s	1263 vs	1343 ms	1386 s	1386 s	$\nu_s(NO_2)$; PA
1321 s	1207 w	1312 w	1357 vw	1357 s	ν(C–C) + ν(C–N) + ν(C–O)
1295 s	1168 w	1263 w	1300 vs	1342 w	In-plane bending
1269 vs		1150 ms	1214 s	1328 s	
1154 vs		1086 s	1171 s	1217 vs	
1065 s			1143 vw	1214 s	
1039 s			1043 s	1171 s	
				1114 s	
				1014 w	
986 s	981 vs	917 vs	971 s	928 s	(C–H) bend
944 ms	851 vs	829 w	900 m	886 s	Aromatic rings vibrations
902 s	752 vs	781 s	857 m	828 s	
887 s		732 s	843 vs	800 s	
855 ms			800 s	757 s	
829 vs			728 w	714 s	
777 ms					
735 s					
682 s	690 vs	703 s	643 w	686 vs	Aromatic rings vibrations of ortho substituted
661 s	569 vs	652 sh	600 w	642 s	Skeletal vibrations
609 s		522 ms	586 vs	586 w	
583 s			543 vs	528 s	
525 s			443 vs	428 s	
425 s					

[a] s, strong; w, weak; m, medium; sh, shoulder; v, very; br, broad.

[b] ν, stretching; δ, bending.

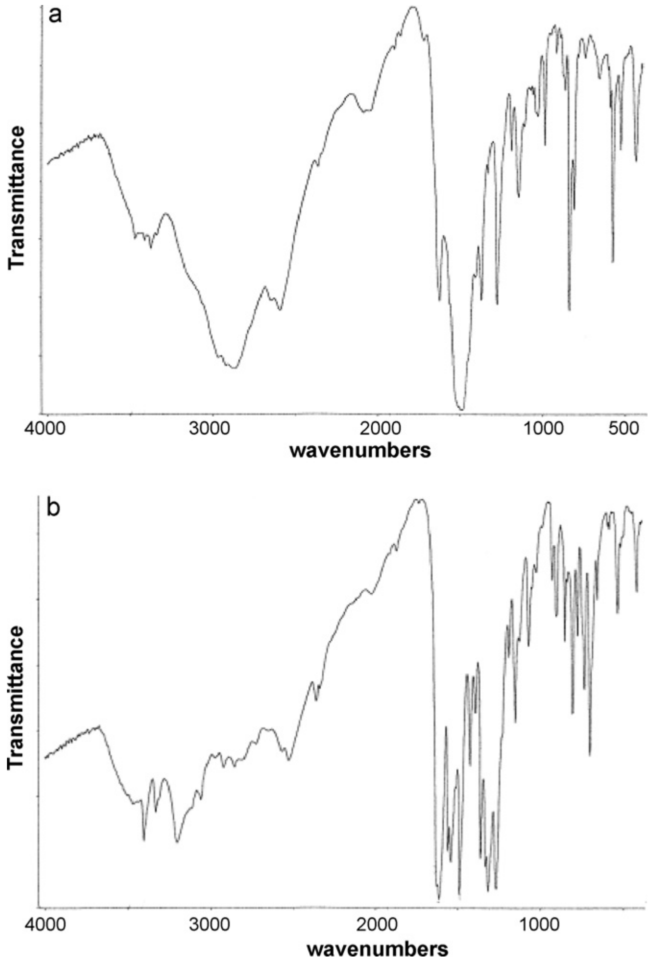

Fig. 4. (a) Infrared spectrum of [(o-TOL)(CA)] CT complex. (b) Infrared spectrum of [(o-TOL)(PA)] CT complex.

and shifted to lower wavenumbers and consequently the intensity was distorted, this results can be summarized as the following explanatory equation;

1625 vs + 1574 s (o-TOL free donor) →
1618 s + 1485 vs (o-TOL/CA complex)
1614 vs + 1557 s (o-TOL/PA complex)

As expected, the bands characteristic for the o-TOL unit in [(o-TOL)(CA)] and [(o-TOL)(PA)] CT-complexes are existed with small changes in band intensities and frequency values. This could be attributed to the expected symmetry and electronic structure changes upon the formation of the CT-complexes.

3.3. 3.3. *^{1}H NMR, ^{13}C NMR and ^{1}H–^{1}H-Cosy spectral studies*

The reaction between chloranilic acid and o-tolidine in methanol carried out in 2:1 ratio through formation of hydrogen bond between –OH of CA and –NH_2 group of o-TOL. The ^{1}H and ^{13}C NMR spectroscopic data (Figs. 5 and 6) proved the formation of symmetrical compound with 6 types of hydrogen protons, five on o-TOL molecule and one for the OH of CA, also, the ^{13}C NMR spectrum (Fig. 6) for the same product showed signals for 10 different carbons 7 for o-TOL molecule and 3 for CA, this means that, presence of axis of symmetry for the formed product (Formula II).

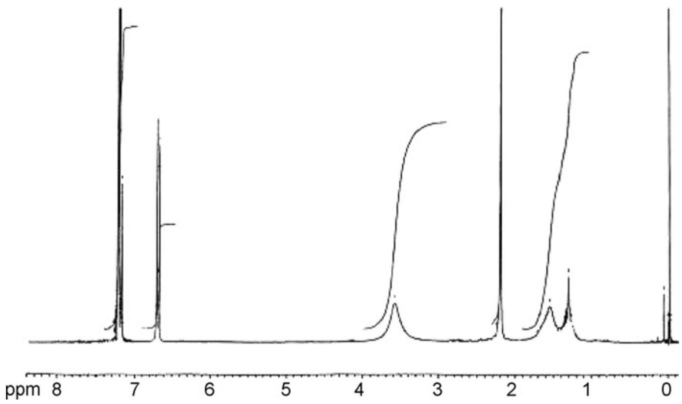

Fig. 5. ^{1}H NMR spectrum of [(o-TOL)(CA)] CT complex.

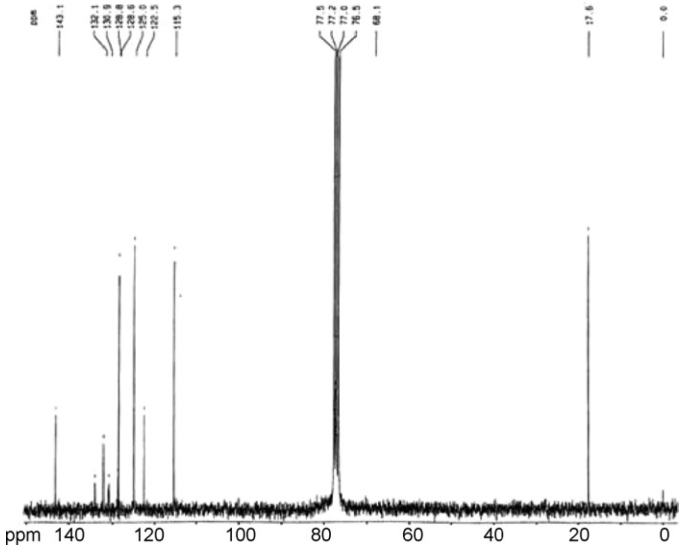

Fig. 6. ^{13}C NMR spectrum of [(o-TOL)(CA)] CT complex.

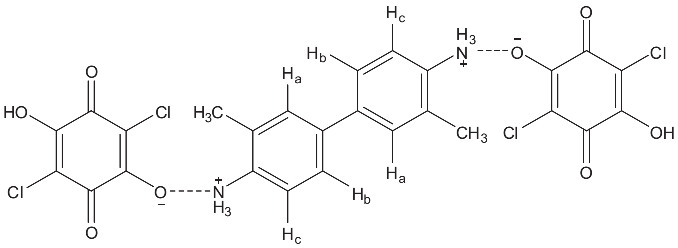

The full analysis recorded is, ^{1}H NMR (Fig. 5) ($CDCl_3$) for symmetrical 2,2′-[(3,3′-dimethylbiphenyl-4,4′-diyl)bis(aminohydroxy)]bis(3,6-dichloro-5-hydroxy-benzo-1,4-quinone), gave a signals at:

$\delta = 1.25$ (br, 2H, 2OH), 1.57 (br, 2H, NH_2), 2.22 (s, 3H, CH_3), 6.73 (d, 1H$_b$, $J = 7.5$ Hz, Ar–H), 7.24 (d, 1H$_c$, $J = 7.5$ Hz, Ar–H), 7.26 (s, 1H$_a$, Ar–H). ^{1}H–^{1}H-Cosy indicates (Fig. 7) that H$_c$ coupled with H$_b$ as ortho coupling as shown in spectrum. ^{13}C NMR ($CDCl_3$); $\delta = 17.6$ (CH_3), 115.3, 122.5, 125.0, 128.6, 128.8, 130.9, 132.1, 134.2 and 143.1 (Ar–C and C=O).

On the other hand, the reaction between picric acid and o-TOL in methanol formed an ionic compound on the bases of hydrogen transfer from picric acid –OH to –NH_2 of o-TOL also in ratio 2:1 PA-to-o-TOL. The spectral studies for ^{1}H, ^{13}CNMR (Figs. 8 and 9) proved formation of symmetrical compound between electron rich molecule, o-TOL, and electron deficient, picric acid.

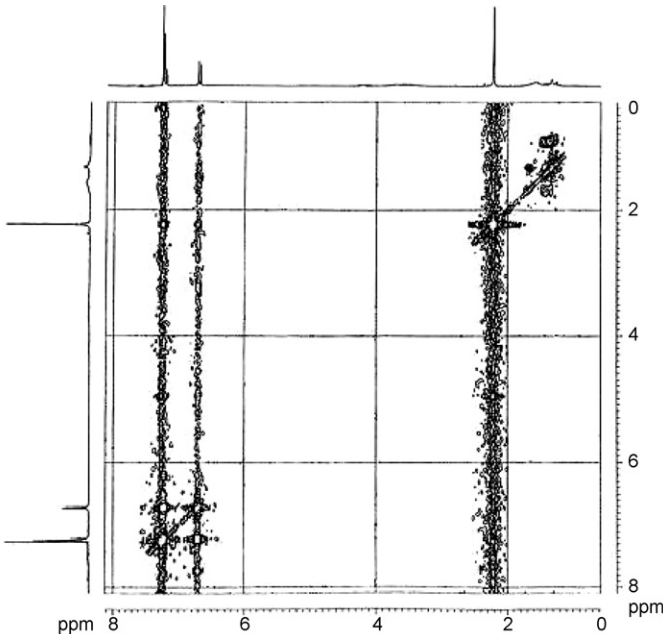

Fig. 7. ^1H–^1H-Cosy spectrum of [(o-TOL)(CA)] CT complex.

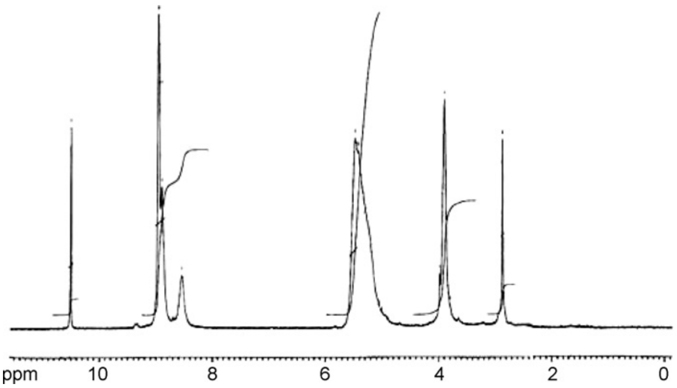

Fig. 8. ^1H NMR spectrum of [(o-TOL)(PA)] CT complex.

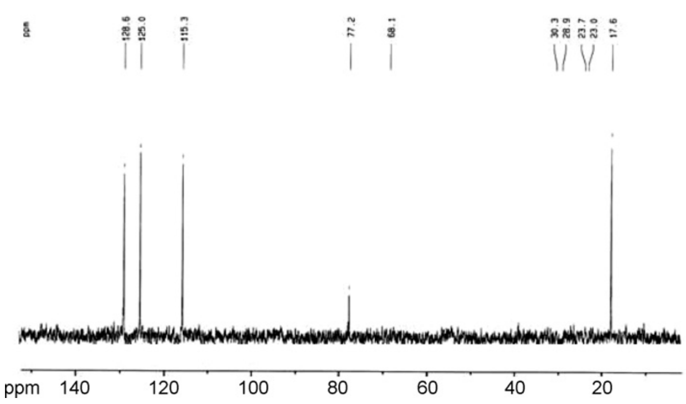

Fig. 9. ^{13}C NMR spectrum of [(o-TOL)(PA)] CT complex.

The formation of ionic NH_3^+ was confirmed by the ^1H NMR (Fig. 8) formed at $\delta = 42$ and disappearance of the signal due to OH proton of picric acid (Formula III).

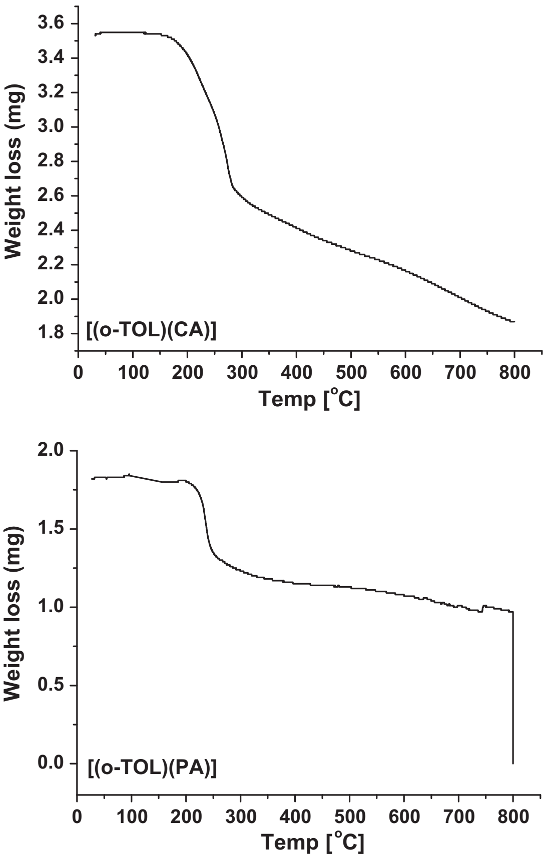

Fig. 10. TG curves of o-TOL CT complexes.

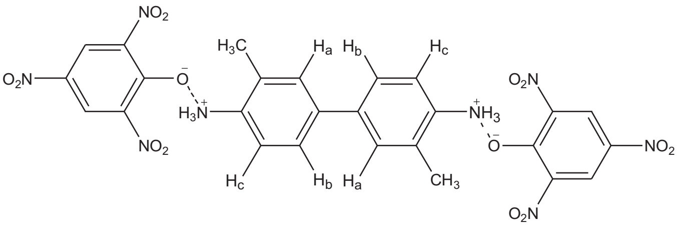

The full analysis recorded is, ^1H NMR ($CDCl_3$) for symmetrical 3,3′-dimethylbiphenyl-4,4′-diaminium di(2,4,6-trinitrophenolate), gave a signals at:

$\delta = 2.87$ (s, 3H, CH_3), 5.42 (br, 3H, NH_3^+), 8.56 (d, $1H_b$, $J = 7.8$ Hz, Ar–H), 8.91 (d, $1H_c$, $J = 7.8$ Hz, Ar–H), 8.89 (s, $1H_a$, Ar–H), 10.5 (s, 2H, Ar–H, picrate).

3.4. Thermogravimetric studies

The thermo gravimetric analysis give an idea about the thermal stabilities of the prepared charge transfer complexes and also show the different in physical behavior between the starting and resulting compounds. TG curves of o-tolidine CT complexes are shown in Fig. 10. The o-TOL donor beginning decomposed at ∼129 °C with maximum decomposition at 244 °C. The thermal decomposition of o-TOL occurs sum in one step which was detected at 244 °C within the range of 200–800 °C corresponding to loss of $C_{12}H_{16}N_2$ organic moiety representing a weight loss of obs = 88.65%, calc = 88.70% then leaving residual carbon as final product.

TG curve of [(o-TOL)(CA)] CT-complex was thermally decomposed in nearly two decomposition steps within the temperature rang 25–800 °C. The first decomposition step (obs = 27.00%, calc = 27.92%) within the temperature range 25–288 °C, may be assigned to the liberation of $2Cl_2 + H_2O + 0.5O_2$ molecules. The

Table 3
Kinetic parameters of [(o-TOL)(CA)] and [(o-TOL)(PA)] CT-complexes.

Complex	n	Parameter					
		E (J mol^{-1})	Z (s^{-1})	ΔS (J mol^{-1} K^{-1})	ΔH (J mol^{-1})	ΔG (J mol^{-1})	r
[(o-TOL)(CA)]							
CR	1	157	2.62×10^{13}	−7.45	152	148	0.9882
HM	1	75.6	4.31×10^{5}	−1.42	71.4	144	0.9975
[(o-TOL)(PA)]							
CR	1	182	4.5×10^{16}	−169.2	178	141	0.9979
HM	1	129	2.78×10^{5}	−241	125	151	0.9990

n = number of decomposition steps.

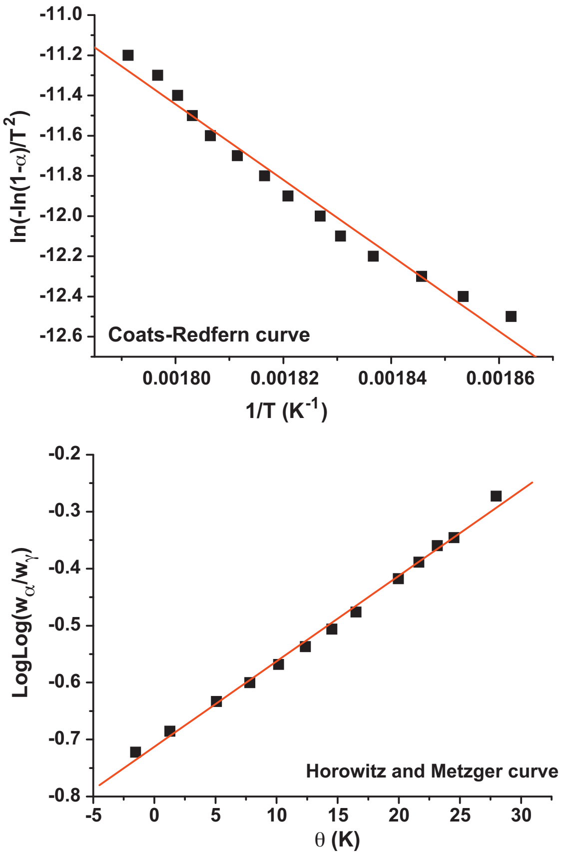

Fig. 11. Kinetic curves of decomposition steps of [(o-TOL)(CA)] complex using Coats and Redfern (CR) and Horowitz and Metzger equations.

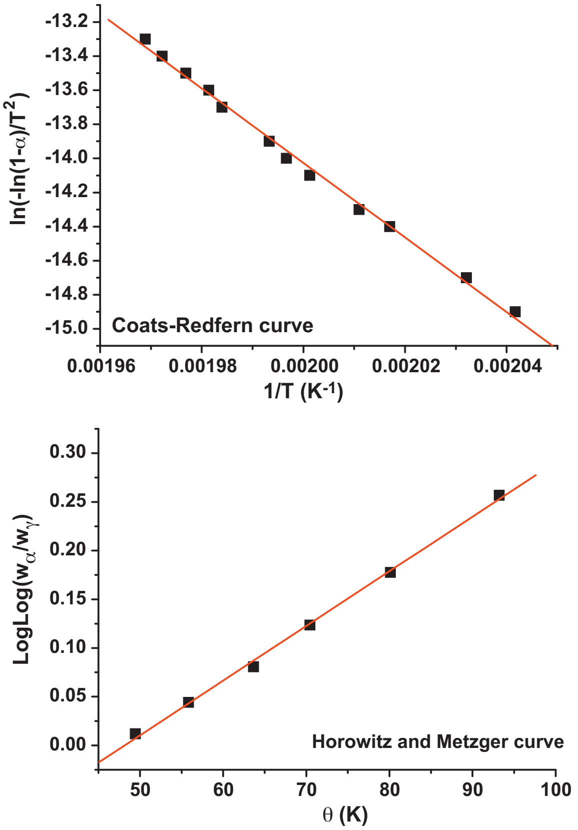

Fig. 12. Kinetic curves of decomposition steps of [(o-TOL)(PA)] complex using Coats and Redfern (CR) and Horowitz and Metzger equations.

second decomposition step found within the temperature range 288–800 °C (obs = 22.00%, calc = 22.52%) which are assigned by the removal of $6H_2O$ and $2NH_3$ molecules with remaining a many carbon atoms as a final residual.

The [(o-TOL)(PA)] CT complex was decomposed thermally in two definite decomposition steps (250 and 516 °C) within the temperature rang 100–800 °C. The first decomposition step (obs = 36.50%, calc = 36.55%) within the temperature range 100–395 °C, may be attributed to the liberation of one molecule of PA and NH_2 group from o-TOL donor. The second decomposition step existed within the temperature range 395–800 °C (obs = 63.50%, calc = 63.45%), which are reasonably by the loss of one molecule of PA and $C_{14}H_{14}N$ organic moiety remnant from o-TOL molecule.

3.5. Kinetic thermodynamic studies

The kinetic studies on thermal process are expected to provide sufficient information regarding Arrhenius parameters *viz.* activation energy (E^*), frequency factor (A), enthalpy of activation (H^*), entropy of activation (S^*), free energy of activation (G^*). From TG data employing Coats–Redfern [32] and Horowitz and Metzger [33] equations various kinetic thermodynamic parameters have been calculated. The kinetic data obtained for the non isothermal decomposition of complexes are given in Table 3 and Figs. 11 and 12. Generally, the value of (A) increases with decrease in E^* and higher value of activation energy suggests the higher thermal stability.

i Coats–Redfern equation is as follows:

$$\mathrm{Ln}\left[\frac{-\ln(1-a)}{T^2}\right] = -\frac{E^*}{RT} + \ln\left[\frac{AR}{\varphi E^*}\right] \tag{8}$$

where α is the fraction of the sample decomposed at time T, where T is the derivative peak temperature, A is frequency factor, R is the gas constant, E^* is the activation energy and φ is the linear heating rate. A plot of left side vs $1/T$ gives a slope for the evaluation of activation energy.

ii Horowitz–Metzger equation is as follows:

$$\log\left[\log\frac{w_\alpha}{w_\gamma}\right] = \frac{E^*\theta}{2.303RT_s{}^2} - \log 2.303 \qquad (9)$$

where $\theta = T - T_s$, $w_\gamma = w_\alpha - w$, w_α = mass loss at the completion of the reaction; w = mass loss up to time t. The plot of $\log[\log(w_\alpha/w_\gamma)]$ vs θ was drawn and found to be linear from the slope of which E^* was calculated.

The entropy of activation, ΔS^*, was calculated from the following equations. The enthalpy activation, ΔH^*, and Gibbs free energy, ΔG^* were calculated from;

$$\Delta H^* = E^* - RT \qquad (10)$$

$$\text{and } \Delta G^* = DH^* - T\Delta S^* \qquad (11)$$

The higher values of 'E^*' and lower values of (A) favor the reaction to proceed slower than normal [34]. The activation energy values (E^*) of CT-complexes arranged with order of thermal stability as: [(o-TOL)(PA)] > [(o-TOL)(CA)].

From the kinetic and thermodynamic data resulted from the TGA curves and tabulated in Table 3, the following outcome can be discussed as follows:

1 The higher values of activation energies of the o-TOL complexes led to thermal stability of the studied complexes.
2 The correlation coefficients of the Arrhenius plots of the thermal decomposition steps were found to lie in the range 0.98–0.99, showing a good fit with linear function.
3 It is clear that the thermal decomposition process of all o-TOL complexes is non-spontaneous, i.e., the complexes are thermally stable.

References

[1] J.R. Peregrina, A. Sánchez-Azqueta, B. Herguedas, M. Martínez-Júlvez, Biochim. Biophys. Acta (BBA): Bioenerg. 1797 (9) (2010) 1638.
[2] S.-L. Wang, J.-M. Lin, S.-E. Shu, C.-Y. Chern, J. Photochem. Photobiol. A: Chem. 210 (1) (2010) 54.
[3] N. Singh, A. Ahmad, J. Mol. Struct. 977 (1–3) (2010) 197.
[4] I.M. Khan, A. Ahmad, J. Mol. Struct. 977 (1–3) (2010) 189.
[5] A. Chakraborty, K.L. Barbu-Debus, A. Zehnacker-Rentien, N. Guchhait, J. Photochem. Photobiol. A: Chem. 213 (2–3) (2010) 164.
[6] K. Takahasi, K. Horino, T. Komura, K. Murata, Bull. Chem. Soc. Jpn. (1993) 66.
[7] P.J. Trotter, P.A. White, Appl. Spectrosc. 32 (1978) 323.
[8] R.A. Marcus, Rev. Mod. Phys. 65 (1993) 599.
[9] H. Duymus, M. Arslan, M. Kucukislamoglu, M. Zengin, Spectrochim. Acta Part A 65 (5) (2006) 1120.
[10] I.M. Khan, A. Ahmad, M. Oves, Spectrochim. Acta Part A 77 (5) (2010) 1059.
[11] M. Pandeeswaran, K.P. Elango, Spectrochim. Acta Part A 75 (5) (2010) 1462.
[12] P. Singh, P. Kumar, A. Katyal, R. Kalra, S.K. Dass, S. Prakash, R. Chandra, Spectrochim. Acta Part A 75 (3) (2010) 983.
[13] C.R. Noller, Textbook of Organic Chemistry, Springer Verlag, 1960.
[14] G. Gangadhar, Chemoshere 32 (2) (1996) 267.
[15] G.M. Malanoski, E.A. Elliot, Epidemiol. Rev. 3 (1981) 203.
[16] G. Pfizenmair, T. Pflaum, Naturwissenschaften 3 (1995) 40.
[17] M.S. Refat, H.M.A. Killa, I. Grabchev, M.Y. El-Sayed, Can. J. Anal. Sci. Spectrosc. 52 (2) (2007) 75.
[18] M.S. Refat, L.A. El-Zayat, Okan Zafer Yeşilel, Polyhedron 27 (2) (2008) 475.
[19] M.S. Refat, H.A. Ahmed, I. Grabchev, L.A. El-Zayat, Spectrochim. Acta 70 (4) (2008) 907.
[20] M.S. Refat, L.A. El-Zayat, Okan Zafer Yeşilel, Spectrochim. Acta Part A 75 (2010) 745.
[21] D.A. Skoog, Principle of Instrumental Analysis, 3rd edn., Saunders College Publishing, New York, USA, 1985 (Chapter 7).
[22] A. El-Kourashy, Spectrochim. Acta 37A (1981) 399.
[23] H. Tsubomura, R.P. Lang, J. Am. Chem. Soc. 86 (1964) 3930.
[24] S.M. Teleb, M.S. Refat, Spectrochim. Acta Part A 60 (7) (2004) 1579.
[25] E.M. Nour, S.M. Teleb, M.A.F. El-Mosallamy, M.S. Refat, South Afr. J. Chem. 56 (2003) 10.
[26] R. Rathone, S.V. Lindeman, J.K. Kochi, J. Am. Chem. Soc. 119 (1997) 9393.
[27] G. Aloisi, S. Pignataro, J. Chem. Soc. Faraday Trans. 69 (1972) 534.
[28] G. Briegleb, Z. Angew. Chem. 72 (1960) 401;
G. Briegleb, Z. Angew. Chem. 76 (1964) 326.
[29] G. Briegleb, J. Czekalla, Z. Physikchem. (Frankfurt) 24 (1960) 237.
[30] A.N. Martin, J. Swarbrick, A. Cammarata, Physical Pharmacy, 3rd ed., Lee and Febiger, Philadelphia, PA, 1969, 344 pp.
[31] L.J. Bellamy, The Infrared Spectra of Complex Molecules, Chapman & Hall, London, 1975.
[32] A.W. Coats, J.P. Redfern, Nature (London) 201 (1964) 68.
[33] H.H. Horowitz, G. Metzger, Anal. Chem. 35 (1963) 1464.
[34] N. Sharma, Archana, M. Thakur, S.S. Bhatt, S.C. Chaudhry, J. Chem. Sci. 119 (4) (2007) 311.